



Impact of electrode sequence on electrochemical removal of trichloroethylene from aqueous solution

Ljiljana Rajic, Noushin Fallahpour, Akram N. Alshawabkeh*

Department of Civil and Environmental Engineering, Northeastern University, 400 Snell Engineering, 360 Huntington Avenue, Boston, MA 02115, United States

ARTICLE INFO

Article history:

Received 24 September 2014

Received in revised form 7 January 2015

Accepted 12 March 2015

Available online 21 March 2015

Keywords:

Trichloroethylene

Groundwater

Reduction

Treatment

ABSTRACT

The electrode sequence in a mixed flow-through electrochemical cell is evaluated to improve the hydrodechlorination (HDC) of trichloroethylene (TCE) in aqueous solutions. In a mixed (undivided) electrochemical cell, oxygen generated at the anode competes with the transformation of target contaminants at the cathode. In this study, we evaluate the effect of placing the anode downstream from the cathode and using multiple electrodes to promote TCE reduction. Experiments with a cathode followed by an anode (C → A) and an anode followed by a cathode (A → C) were conducted using mixed metal oxide (MMO) and iron as electrode materials. The TCE removal rates when the anode is placed downstream of the cathode (C → A) were 54% by MMO → MMO, 64% by MMO → Fe and 87% by Fe → MMO sequence. Removal rates when the anode is placed upstream of the cathode (A → C) were 38% by MMO → MMO, 58% by Fe → MMO and 69% by MMO → Fe sequence. Placing the anode downstream of the cathode positively improves (by 26%) the degradation of aqueous TCE in a mixed flow-through cell as it minimizes the influence of oxygen generated at the MMO anode on TCE reduction at the cathode. Furthermore, placing the MMO anode downstream of the cathode neutralizes pH and redox potential of the treated solution. Higher flow velocity under the C → A setup increases TCE mass flux reduction rate. Using multiple cathodes and an iron foam cathode up stream of the anode increase the removal rate by 1.6 and 2.4 times, respectively. More than 99% of TCE was removed in the presence of Pd catalyst on carbon and as an iron foam coating. Enhanced reaction rates found in this study imply that a mixed flow-through electrochemical cell with multiple cathodes up stream of an anode is an effective method to promote the reduction of TCE in groundwater.

Published by Elsevier B.V.

1. Introduction

Trichloroethylene (TCE) is a chlorinated solvent that has been widely used in industrial cleaning solutions and as a “universal” degreasing agent due to its unique properties and solvent effects. TCE is among 29 of the substances most commonly found at the USEPA (United States Environmental Protection Agency) Superfund sites [1]. At many TCE spill sites, residual amounts of TCE persist in a pure liquid phase (known as dense, non-aqueous-phase liquids, DNAPLs) within pore spaces or fractures [2]. The slow dissolution of residual TCE results in a contaminated plume of groundwater. Because of potential health effects, the USEPA has set Maximum Contaminant Levels (MCLs) for TCE in drinking water at very low concentrations (5 µg L⁻¹).

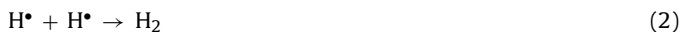
Methods that have been proposed to remove TCE from groundwater include microbial degradation [3–5], photochemical oxidation [6,7], sonochemical processes [8–10], and chemical reduction via zero-valent iron (ZVI) [12–15] or palladium-based materials [16–22]. Microbial processes suffer from long reaction time and limiting effects. Due to the thermodynamic instability of ZVI in water, changes in environmental conditions encourage the development of a corrosion surface layer. The formation of this surface layer can inhibit electron transfer and catalytic hydrogenation between any contaminants and the iron. A combination of ultraviolet light (UV) with ozone, hydrogen peroxide, Fenton's reagent or oxalate-complexes can be effective in degrading TCE [22–28]. Disadvantages of these methods include limitation of dissolved oxygen mass transfer, use of expensive chemicals, high capital costs, lack of mobility of the equipment and the potential formation of toxic byproducts.

Electrochemical treatment offers a significant potential for in situ transformation of TCE [29–31]. Due to their chemical nature,

* Corresponding author. Tel.: +1 617 373 3994.

E-mail address: aalsha@coe.neu.edu (A.N. Alshawabkeh).

attention was focused on cathodic reduction and dehalogenation of TCE and other highly oxidized chlorinated aliphatic hydrocarbons [11,32–37]. Transformation of these compounds at the cathode surface may occur through both direct and indirect mechanisms. Direct reduction occurs by electron tunneling or by formation of a chemisorption complex of the compound with the cathode material [38,39]. Indirect reduction, or hydrodechlorination (HDC), occurs via a reaction with atomic hydrogen and is the main reduction mechanism at hydrogen formation potentials. Atomic hydrogen adsorbed on the cathode can reduce organic compounds through formation of chemisorbed hydride complexes [39]. The reactions that occur at the cathode surface include:



Reduction by HDC is fast on cathodes with low hydrogen overpotentials, such as platinum and palladium, but much slower on metals with high hydrogen overpotentials, such as iron. In some cases, using larger electrode surface area is sufficient in increasing the rate of hydrogen formation [40]. Noble metals (e.g., Ag, Pt and Pd) are often used as working electrodes [41–43] because of the capability of absorbing hydrogen which promotes HDC [44]. Various materials, such as activated carbon fiber/cloth/felt, reticulated vitreous carbon and carbon nanotubes, meshed Ti, Ti/TiO₂ nanotubes, foam Ni, foam Fe and Ebonex® were frequently used as cathode substrates supporting Pd catalyst because of the penetrability and advantage for mass transfer in the dechlorination process [44–49]. Palladized electrodes were used for removal of TCE [37,50–52], chlorinated phenols [45,52,53], carbon tetrachloride [37], 4-chlorobiphenyl and 2,4,5-trichlorobiphenyl [47]. These were evaluated in the reactors with divided electrolytes where the anodes and cathodes are separated by ion exchange membranes.

Electrochemical treatment of groundwater in a reactor with mixed anolyte and catholyte has advantages over reactors with divided electrolytes because of lower energy requirements and easier installation and maintenance in the field [33]. In a mixed electrolyte, both reduction and oxidation processes could be optimized for efficient removal of highly oxidized contaminants [53–59]. Electrode materials and electrode arrangements could be selected to achieve specific conditions for the desired redox reactions [29,30,33–35]. For example, a two electrode mixed electrolyte system using an iron anode was successfully implemented for reduction of TCE and other contaminants [34]. The reduction potential of oxygen (1.229 V vs. SHE, standard hydrogen electrode) is higher than that of TCE (0.42 V vs. SHE from TCE to *cis*-DCE) so oxygen is reduced at the cathode along with the H₂O rather than TCE [34]. Employing Fe anode produces ferrous ions instead of oxygen gas and supports the reduction mechanism (Reaction (4)),



Using iron anodes in undivided electrochemical cells eliminates the competition between oxygen and contaminants for reduction at the cathode but may cause precipitation and an increase in pH [34]. Optimizing electrode sequence is an alternative approach to promote the reduction of contaminants at the cathode in a mixed electrochemical cell by minimizing the effects of the anodic processes. We evaluated electrode sequences with an anode downstream from the cathode to diminish the interaction between oxygen and the cathode, therefore promoting TCE reduction. Further, we evaluated using multiple cathodes (iron foam and perforated cast iron), increasing cathode surface area (iron foam cathode) and using Pd catalyst in the cathode vicinity (Pd on

alumina, carbon or iron foam) to enhance the reduction of TCE by the proposed electrode sequence.

2. Materials and methods

All chemicals used in this study were analytical grade. TCE [99.5%] and *cis*-dichloroethylene (*cis*-DCE, 97%) were purchased from Sigma–Aldrich. Calcium sulfate was purchased from JT Baker, oxalic acid (anhydrous, 98%) from Acros Organics, sodium chloride, sodium acetate and sodium bicarbonate from Fisher Scientific. Ti/mixed metal oxide (MMO) mesh (3 N International) and gray cast iron (McMaster–Carr) were used as electrode materials. The Ti/MMO electrode consists of IrO₂ and Ta₂O₅ coating on titanium mesh with dimensions of 3.6 cm diameter by 1.8 mm thickness. Perforated cast gray iron disk (Ø=3.6 cm) and iron foam (45 pores per inch, PPI, 98% iron and 2% nickel, Aibixi Ltd. China) perforated with 0.5 cm holes were used as electrodes. Deionized water (18.2 MΩ cm) obtained from a Millipore Milli-Q system was used in all the experiments. Palladium catalyst supported on alumina pellets, Pd/Al (0.5 wt.% Pd, Sigma–Aldrich) with average size of 3.2 mm and on 4–8 mesh activated carbon (4.75–2.36 mm), Pd/C (1 wt.% Pd, Acros Organics) was used. Cast iron electrodes were not subjected to palladization since the high surface area is the most important characteristic of catalyst supporting material [47]. The iron foam electrodes were etched by diluted HCl (10 wt.%) and washed with deionized water. Prior to palladization [52], the iron foam electrodes were immersed in 1 M HCl to remove any foreign metal and the surface oxide layers. After a thorough rinsing of the electrodes with deionized water, the electroless plating of Pd was performed in a closed beaker with a PdCl₂ solution (to ensure 10 mg Pd coating) and 0.1 M HCl, and rotated at 300 rpm until the dark orange PdCl₂ solution turned colorless. The procedure was always performed under exactly the same conditions to ensure the deposition of the same amount of Pd and to achieve the same surface quality on each plate. After palladization, the iron plates were rinsed with deionized water. The exact amount of deposited Pd was calculated from the concentrations of the PdCl₂ solution measured spectrophotometrically at 480 nm, before and after electro plating. Scanning electron microscope (SEM) (Hitachi S-4800 FESEM) was used to prove Pd deposition on the foam iron cathode surface.

TCE and *cis*-DCE concentrations were measured by a 1200 Infinity Series HPLC (Agilent) equipped with a 1260 DAD detector and a Thermo ODS Hypersil C18 column (4.6 × 50 mm). The mobile phase was a mixture of acetonitrile and water [60:40, v/v] at 1 mL min^{−1}. 2 mL samples were collected from the sampling ports for analysis. Concentration of VC in aqueous solution was measured using 8610GC Gas Chromatograph with purge-trap system (SRI, USA), photoionization detector, and MXT-VOL stationary column. The purge-trap autosampler was equipped with carbon-sieve trap and Tenax trap. 50 µL of water sample was injected in 5 mL of deionized water in glass tubes and loaded into the 10-port autosampler. The GC was programmed at 40 °C for 6 min, then ramped to 60 °C in 2 min, and held at 60 °C for 10 min.

Analyses of chloride ions, acetates and oxalates were performed using an ion chromatography (IC) instrument (Dionex 5000) equipped with an AS20 analytical column. A KOH solution (35 mM) was used as a mobile phase at a flow rate of 1.0 mL min^{−1}. The chlorides mass balance during the treatment was calculated to validate TCE reduction. pH and oxidation–reduction potential (ORP) of the electrolyte were measured by pH meter and ORP meter with corresponding microprobes (Microelectro, USA). The microprobes allow the measurement on these parameters using a small amount of liquid (≈0.2 mL).

The electrochemical reactor with two and three electrodes is shown in Fig. 1. The experimental conditions are given in

Table 1

Experimental conditions (60 mA current intensity, 0.25 cm min⁻¹ flow velocity and 5.3 mg L⁻¹ initial TCE concentration).

Electrode arrangement ^a	Electrode material	Catalyst type and mass (g)
(C → A)	MMO → Fe	–
(C → A)	Fe → MMO	–
(A → C)	MMO → Fe	–
(C → A)	Fe foam → MMO	–
(C → A)	Fe foam.Pd → MMO	–
(C → A)	Fe → MMO	Pd on Al; 2 g
(C → A)	Fe → MMO	Pd on Al; 5 g
(C → A)	Fe → MMO	Pd on C; 1 g
(C → C → A)	Fe → Fe → MMO	–
(C → C → A)	Fe → Fe → MMO	^b Pd on Al; 2 g
(C → C → A)	Fe → Fe → MMO	Pd on Al; 5 g
(C → C → A)	Fe → Fe → MMO	Pd on C; 1 g
(C → C → A)	Fe foam → Fe → MMO	–
(C → C → A)	Fe foam → Fe → MMO	Pd on C; 1 g

^a A-anode and C-cathode are placed in order E1 and E2, and E1, E2 and E3

^b In the three electrode system catalyst is placed on E1

Table 1. The performance of Fe/MMO (C → A) electrodes arrangement was tested under different current intensities (30 mA, 60 mA and 90 mA), flow velocities (0.25 cm min⁻¹ and 0.5 cm min⁻¹), initial TCE concentrations (2.7 ppm, 5.3 ppm and 8 ppm) and different anode-cathode spacing (2.5 cm and 5 cm).

In the three electrode system (with two cathodes), the current was split by the rheostat, allowing the same current (30 mA) to pass through E1 and E2 cathodes. Two cathodes (iron foam and perforated cast iron) were used to increase TCE retention time within the reducing zone. A vertical acrylic column (Ø = 3.8 cm; H = 10 cm) was used as an electrochemical flow-through reactor. Electrode and sampling port locations are shown in Fig. 1. A layer of glass beads followed by a layer of the desired amount of Pd catalyst (when used) were placed directly on E1 or E2.

Synthetic groundwater was prepared by dissolving 413 mg L⁻¹ sodium bicarbonate and 172 mg L⁻¹ calcium sulfate in deionized water. The concentrations of bicarbonate ions and calcium ions are representative of groundwater from limestone aquifers, resulting in electrical conductivity of 800 to 920 µS cm⁻¹. Excess TCE was dissolved into 18.2 MΩ cm high-purity water to form a TCE saturated solution (1.07 mg mL⁻¹ at 20 °C), which was used as stock solution for preparing aqueous TCE solutions. The feedstock solution was stored in a common Tedlar® bags. The headspace in the bag was minimized to limit TCE losses to the gas phase. The initial pH of the contaminated synthetic groundwater was 8 ± 0.3 and the initial ORP value was 210 ± 5 mV. The temperature was kept constant at 20 °C. Darcy's velocities were selected as 0.25 cm min⁻¹ (2.8 mL min⁻¹) and 0.5 cm min⁻¹ (5.6 mL min⁻¹). A constant flow velocity was maintained by a peristaltic pump (Cole Parmer, Masterflex C/L). A constant current intensity during treatments was

Table 2

Calculated pseudo-first-order rate constants, TCE removal efficacies for 5.3 ppm TCE degradation.

Electrode setup	Pseudo-first-order rate, k (min ⁻¹)	Removal (%)
MMO → Fe (C → A)	5.1 × 10 ⁻³	64
Fe → MMO (C → A)	7.5 × 10 ⁻³	87
MMO → Fe (A → C)	3.4 × 10 ⁻³	69
Fe → MMO (A → C)	6.1 × 10 ⁻³	58

applied by an Agilent E3612A DC power supply. The experiments were conducted for 180 min and electrolysis steady state conditions were assumed when the change in concentration is less than 0.5% per minute which accounts for other TCE losses, such as adsorption or volatilization.

TCE removal was calculated by the following equation:

$$\% \text{removal} = \frac{C_0 - C_t}{C_0} \times 100 \quad (1)$$

where C_0 is the initial TCE concentration (mg L⁻¹) and C_t is TCE concentration at a defined time during treatment (mg L⁻¹).

We calculated the pseudo-first-order reaction rate constants under flow conditions by including the transport and transformation rates. The commonly used pseudo-first-order reaction kinetics model ($\ln C_0/C = kt$) resulted in good correlation coefficients ($R^2 = 92\text{--}97\%$) when modeling TCE transformation.

3. Results and discussion

3.1. The two electrode system for TCE removal

The influence of electrode sequence (C → A or A → C) and electrode material on TCE removal was tested in the flow-through system (Fig. 2) using combinations of Fe and MMO electrodes (Table 1). TCE removal rates and pseudo-first-order rate constants for the TCE decay are summarized in Table 2. Using only MMO electrodes, the C → A arrangement produced 54% removal rate versus 34% for the A → C arrangement. The C → A arrangement positively affects TCE removal compared to the A → C arrangement regardless of the electrode materials used. Control experiments were performed to evaluate the loss of TCE due to evaporation and sorption onto cathodes and/or reactor material. For the concentration tested (5.3 ppm) TCE loss was less than 3.0% after 180 min of flow (Fig. 2a).

The MMO anodes are active types of anodes with strong interactions with hydroxyl radicals formed on their surfaces, low oxygen overpotentials and, therefore, low efficiency to remove organics [60]. Although, it was reported that MMO anode enables TCE oxidation (Reaction (5) and (6)) [31], oxygen evolution (Reaction (7)) significantly competes with the TCE oxidation [60], especially under the current applied in this study (60 mA). The O₂ that formed

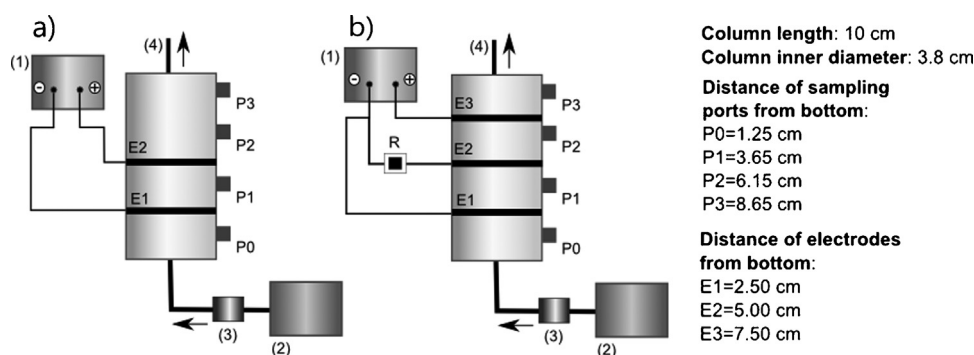


Fig. 1. A schematic of the electrochemical flow-through reactor: (a) the two electrode system (1) DC source; E1 and E2 are electrodes; and (b) the three electrode system (1) DC source; R is rheostat; E1 and E2 and E3 are electrodes; P0, P1, P2 and P3 are sampling ports; (2) Tedlar® bag with synthetic groundwater, (3) peristaltic pump and (4) effluent.

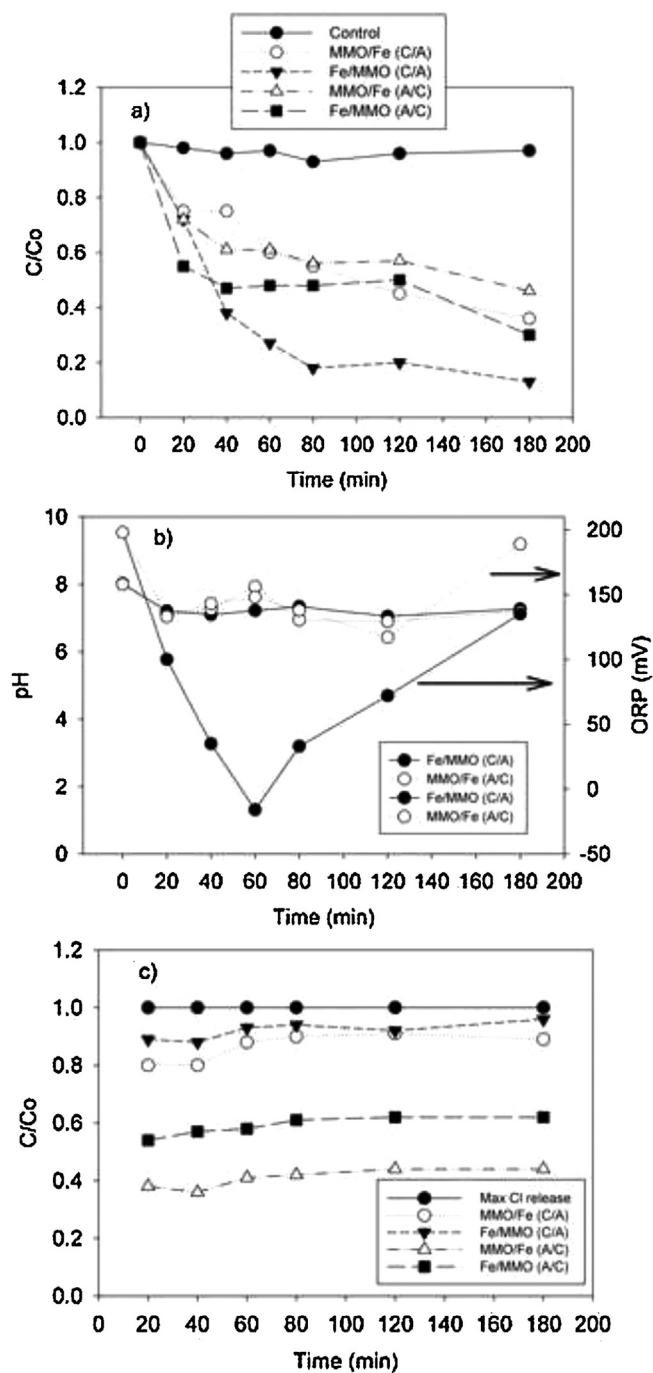
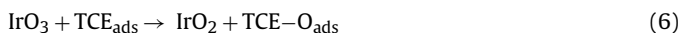
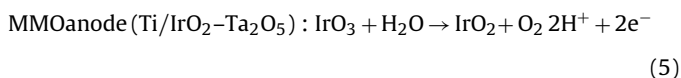


Fig. 2. (a) TCE removal from groundwater in the two electrode flow-through system; (b) the effluent ORP and pH profile and (c) chloride mass balance during the treatment (60 mA current intensity, initial TCE concentration: 5.3 ppm, velocity: 0.25 cm min⁻¹ and electrode distance of 2.5 cm).

on the anode surface was reduced at the cathode along with the H₂O rather than TCE. However, the processes on the MMO anode are beneficial for maintaining the pH and ORP values of the treated water. Protons produced at MMO are driven by flow (and electromigration) toward the cathode and are neutralized by hydroxyl ions generated at the cathode. This minimizes potential contribution of protons to HDC (Fig. 2).



In the arrangement with Fe/MMO (C → A), the effect of O₂ formed at the anode (downstream) on reduction of TCE at the cathode (upstream) is negligible. As the reduction is the favorable degradation pathway for highly oxidized chemicals like TCE, this causes an increase in the overall removal of TCE. It is also evident that the Fe cathode performs better than the MMO cathode for TCE transformation. The Ti/MMO electrodes are reported as an effective cathode substrate for degradation of TCE [36]. However, at the surface of the MMO cathode, hydrogen interacts with the titanium substrate and forms titanium hydride. This reduces the hydrogen available for HDC and therefore decreases MMO cathode activity.

The Fe anode in the C → A setup improves TCE removal. This supports the studies on the influence of the anode on TCE removal in a mixed electrochemical cell [35]. Fe anodes improve TCE reduction as less oxygen is formed and a reducing environment is produced. Formation of iron precipitates occurs in this system.

Effluent pH did not show significant changes after treatment by an MMO anode (Reaction (3)) downstream of the Fe cathode (Fig. 2). Effluent ORP values during the C → A treatment changed during treatment (Fig. 2). The final effluent ORP after C → A was 138 mV. Changes in measured concentration of chloride ions during C → A treatment with MMO anode downstream of a Fe cathode correspond to the calculated chloride released from TCE removal (Fig. 2c). The chlorides balance is presented as normalized concentration to the calculated chloride released from TCE removed. No chlorinated intermediate products such as *cis*-DCE and vinyl chloride were detected in the effluent. Neither acetates nor oxalates formed during the treatment. Given its volatile nature, it is possible that gas stripping would contribute to TCE removal through purging. However, stripping rates will not be affected by the order of the electrodes which affects TCE removal in this study. Further, oxygen formation at the MMO anode would produce more TCE removal by stripping than the Fe anodes, which is not the case in this study. Finally chloride mass balance confirms TCE transformation rather than removal by stripping. Therefore the effect of stripping is considered limited in this study.

3.1.1. The influence of flow rate on TCE removal

The electrode distance influences TCE removal rates. Under a velocity of 0.25 cm min⁻¹ and 60 mA current, the overall removal rate decreased from 87% to 65% when electrode distance was increased from 2.5 cm to 5 cm (initial TCE concentration of 5.3 ppm). Increasing electrode spacing increases the electrical resistance and the cell voltage which adversely affects the removal [61,62]. Accordingly, all experiments were conducted with electrode distance of 2.5 cm.

Increasing flow velocity in the flow-through system increases mass transport, and the efficiency of TCE removal will depend on the mass flux rates relative to the electric charge. A decrease in TCE removal from 87% to 56% is observed when flow velocity increased from 0.25 cm min⁻¹ to 0.5 cm min⁻¹ at a current intensity of 60 mA and initial TCE concentration of 5.3 ppm. Higher flow velocity decreased TCE removal. This is consistent with the literature [21,62]. Mass flux reduction rates (R_{TCE}) were calculated as $R_{\text{TCE}} = q \Delta C_{\text{TCE}}$, where q is the volumetric flux of water through the column (L min⁻¹ m⁻²), and ΔC_{TCE} (mg L⁻¹) is the change in TCE concentration between influent and effluent at defined time. The reduction rate increases with increasing total charge applied (i.e. total charge over time) under a constant current (constant rate of charge supplied per time) (Fig. 3). R_{TCE} relative to the electric charge increases with flow velocity increase due to the increase in

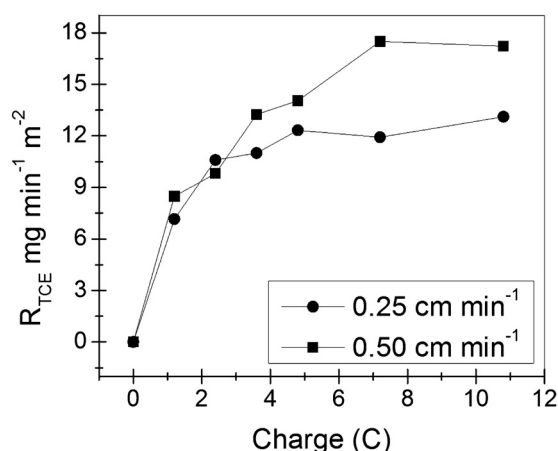


Fig. 3. The rate of TCE mass flux reduction relative to charge (C) in the flow-through system.

TCE mass flux and higher mass transfer associated with the fluid flow.

3.1.2. The influence of initial TCE concentration and current intensity on TCE removal

The electrochemical $C \rightarrow A$ setup was evaluated for different initial TCE concentrations ranging from 2.7 ppm to 8.0 ppm under a current intensity of 60 mA and a flow velocity of 0.25 cm min^{-1} . TCE removal was 99%, 87% and 51% for the initial TCE concentrations of 2.7 ppm, 5.3 ppm and 8.0 ppm, respectively. The loss of TCE in the control experiments was: 2.3%, 3.0% and 3.4%, respectively. This indicates that TCE degradation was not affected by TCE evaporation, sorption onto cathodes or reactor material. Higher initial TCE concentration favors electron transfer for the electroactive species than the background reactions. However, the process will depend on the ratio of mass flux relative to current density. Although the charge flux and retention time are sufficient at low flow rates, the small surface area of the cast iron cathode and agitation at the electrodes surface due to hydrogen gas evolution adversely affect the removal. As the concentration increases under the same flow velocity, the demand for charge transfer increases. Since the current stays constant, the charge is not sufficient for full transformation. Accordingly, the removal rate decreases with increasing concentrations (Fig. 4).

The influence of current on TCE degradation was examined. The experiments were conducted under 30 mA, 60 mA and 90 mA with

Table 3

Calculated pseudo-first-order rate constants and TCE removal efficacies for 5.3 ppm TCE degradation.

Electrode setup	Pseudo-first-order rate constant, k (min^{-1})	Removal (%)
Fe \rightarrow MMO ($C \rightarrow A$)	7.5×10^{-3}	87
Fe foam \rightarrow MMO	1.2×10^{-2}	90
Fe \rightarrow Fe \rightarrow MMO ($C \rightarrow C \rightarrow A$)	1.8×10^{-2}	89
Fe with Pd/C \rightarrow MMO	9.9×10^{-2}	>99
Fe with Pd/A \rightarrow MMO	9.1×10^{-3}	84
Pd/Fe foam cathode \rightarrow MMO	3.3×10^{-2}	>99

initial TCE concentration of 5.3 ppm and under 0.25 cm min^{-1} flow velocity. The final TCE removal rates were 67%, 87% and 51% and pseudo-first-order reaction rate constants were $1.4 \times 10^{-3} \text{ min}^{-1}$, $7.5 \times 10^{-3} \text{ min}^{-1}$ and $5.2 \times 10^{-3} \text{ min}^{-1}$ under 30 mA, 60 mA and 90 mA, respectively. TCE removal increased under 60 mA compared to 30 mA due to the charge increase. However, under current intensity of 90 mA, TCE removal rate decreased. This is due to the higher rate of gas (hydrogen and oxygen) bubbles formation which covers the electrode surface [63]. This adversely affects the availability of electrode surface to degrade TCE. While increasing the electric current increases removal rate, there is an optimum value beyond which TCE removal efficiency decreases. The results also confirm the limited effect of stripping as TCE removal decreases with higher gas production under 90 mA (higher current).

3.1.3. Improving the reduction process in the $C \rightarrow A$ system

To improve performance, we evaluated the impact of using multiple cathodes and the presence of Pd catalyst on the TCE reduction process in the $C \rightarrow A$ sequence. The utilization of multiple cathodes (Fe/Fe/MMO as $C \rightarrow C \rightarrow A$) and a foam iron cathode were examined to improve the performance. Higher electrode surface area (i.e., foam electrodes) improves the transformation of contaminants [36,44,52]. Higher electrode surface area increases the interaction between the electrode surface and TCE and improves hydrogen formation at the cathode [40]. Increasing hydrogen formation accelerates formation of nascent hydrogen and reaction with protons and other reducible substances. The multiple cathodes (Fig. 1) increase the contact surface as well as the retention time for TCE reduction. The current was equally split between the two cathodes (30 mA to E1 and 30 mA to E2). Although the final removal was high in all arrangements, the removal rate increased with both foam and Fe/Fe/MMO ($C \rightarrow C \rightarrow A$) arrangements (Table 3). The removal rate after the first 20 min of the treatment significantly increased (nearly doubled) when multiple cathodes were used. The final TCE removal

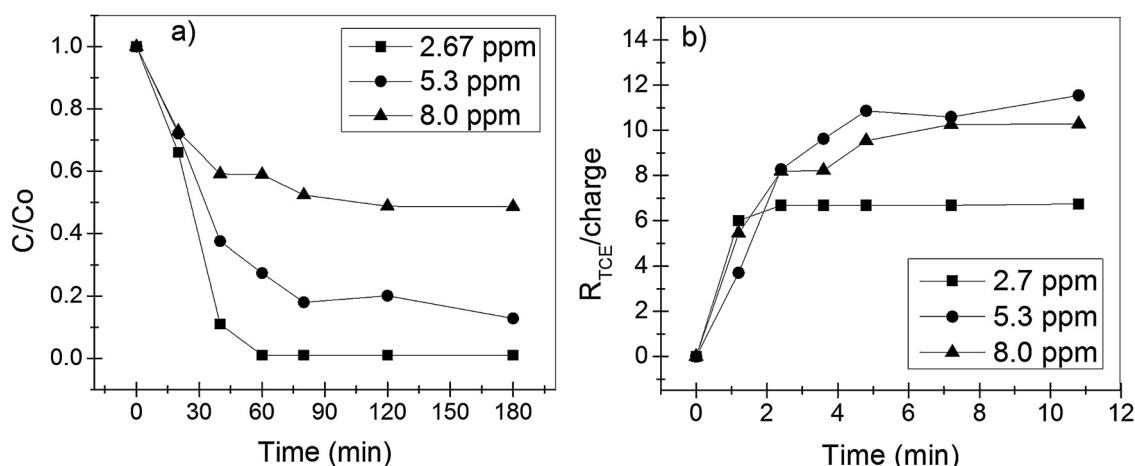


Fig. 4. TCE concentration decay (a) and TCE mass flux rate relative to charge (C) during treatment in the two electrode flow-through system.

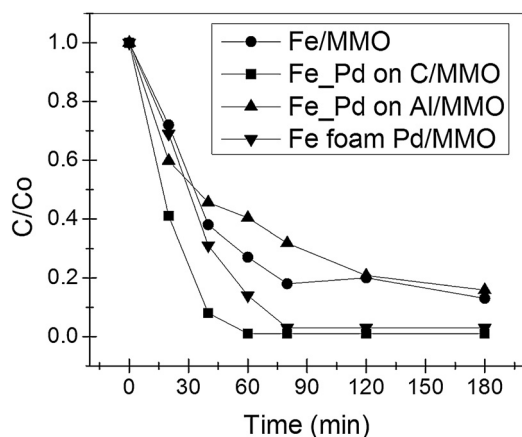


Fig. 5. The influence of Pd supporting material on TCE removal in the two electrode system.

was similar to the one achieved by the Fe/MMO (C → A) setup after 120 min of treatment. Bipolar effect was observed when multiple cathodes were used and precipitation occurred (401 mg). In the bipolar mode the middle iron electrode (E2 cathode) is polarized so the side parallel to E1 acts as anode (Reaction (2)).

Noble metal catalysts (Pd, Pt, Ag) reduce hydrogen overpotential by lowering the activation energy and affecting the overall rate of reaction. They absorb hydrogen which promotes indirect HDC and maintain a high surface concentration of hydrogen [44]. Introducing Pd catalyst in the C → A setup is an advantage. In the A → C setup, Pd catalyzes the formation of H₂O₂ or H₂O on the cathode (depending of the pH at the cathode surface) due to the oxygen presence. The catalyst used in this study was in the form of Pd pellets on

alumina (Pd/Al) and carbon mesh (Pd/C) as well as coating on an iron foam cathode (Fig. 5). The amount of Pd used in each form was 10 mg. The removal efficacies achieved with and without Pd/Al and Pd/C are shown in Table 3. The mechanism of the Pd-catalyzed HDC is that Pd activates molecular hydrogen by the formation of the covalent adatom Pd–H, which attacks the C–Cl bond or any double bond in the substrate molecule [65,66].

More than 99% of TCE was removed after 60 min of treatment when Pd/C was used as cathode. The fact that the Pd/C presence increases removal indicates that sufficient hydrogen for HDC is produced on cast iron. Carbon is of interest as a catalyst support because of the high surface area, high porosity and low reactivity. It was previously shown that Pd/C is more efficient for the HDC process than Pd/Al [67]. High activity of Pd/C can be explained by a high dispersion of impregnated metal due to a porous carbon network allowing hydrogen and TCE dispersion. The other proposed mechanism is organic substance adsorption on the carbon surface [67]. However, the control experiment proved that there was no adsorption/removal during experiments using Pd/C (and Pd/Al). Limited TCE adsorption on carbon is due to the surface polarity of carbon surfaces that results from hydrophilic surface sites. These polar sites act as the growing centers of water clusters and hinder removal of hydrophobic substances by preventing their access to the micropores, where the majority of the carbon surface area for adsorption is located. Water cluster formation is particularly important for adsorption at low concentrations [68]. TCE removal was not affected by the Pd/Al presence. This is probably due to the insufficient interaction between the hydrogen bubbles generated under 60 mA (referring to their size) and the Pd sites on alumina.

Pd deposition on the foam electrode was proven by scanning electron microscope (Fig. 6) and calculating the deposited amount from the concentrations of the PdCl₂ solution before and after electrodeless plating. When palladized foam cathode was used, more than

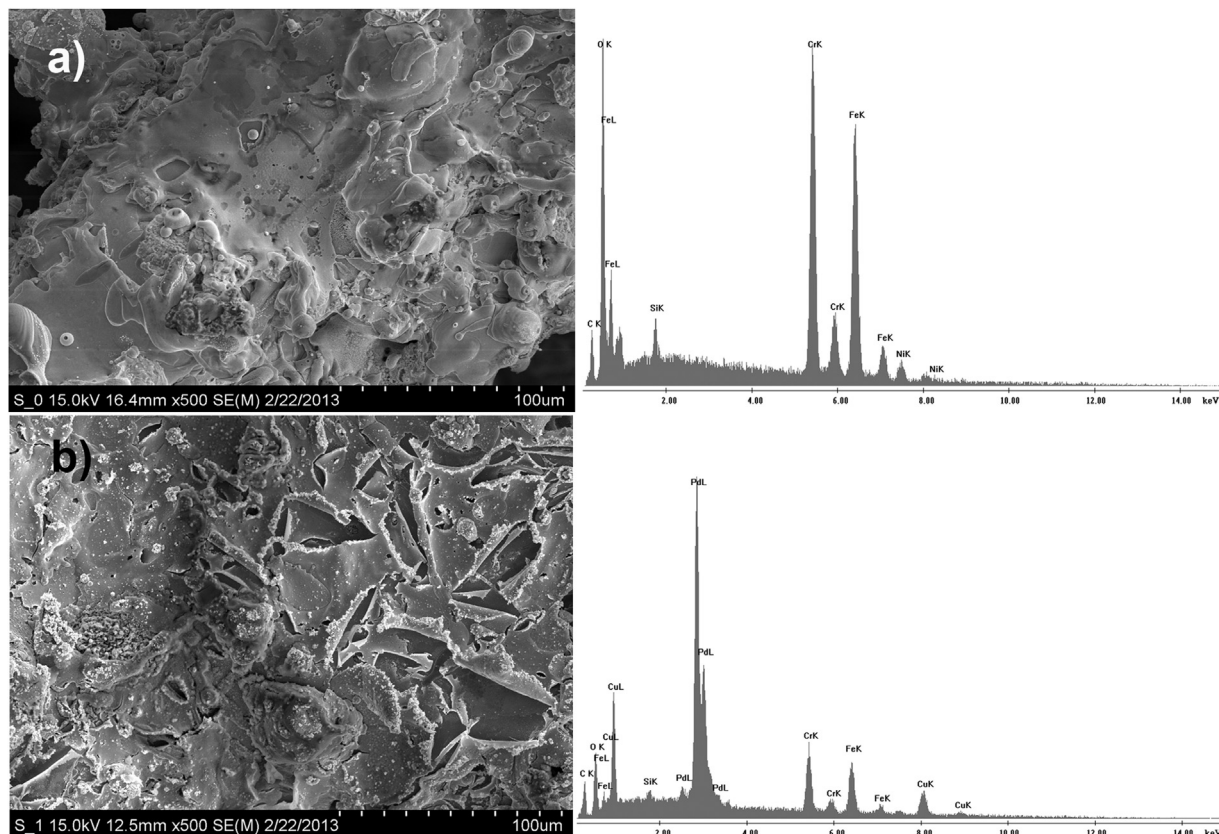


Fig. 6. Scanning electron microscope image of Fe foam cathode (a) before and (b) after palladization.

Table 4

The pseudo-first-order rate constants and TCE removal efficacies for 5.3 ppm TCE degradation in the three electrode system.

Electrode setup	Pseudo-first-order rate constant, k (min^{-1})	Removal (%)
Fe \rightarrow Fe \rightarrow MMO (C \rightarrow C \rightarrow A)	1.8×10^{-2}	89
Fe foam \rightarrow Fe \rightarrow MMO	2.5×10^{-2}	87
Fe with Pd/C \rightarrow Fe \rightarrow MMO	1.5×10^{-1}	>99
Fe with Pd/Al \rightarrow Fe \rightarrow MMO	4.4×10^{-2}	>99
Pd/Fe foam cathode \rightarrow Fe \rightarrow MMO	3.5×10^{-2}	>99

99% of TCE was removed after 80 min of treatment (Table 3). There are three possible HDC mechanisms on palladized cathodes: direct electroreduction, dechlorination at palladium surfaces and dechlorination at palladium-substrate interface [36,44,52]. In the first mechanism, the reductive dechlorination is a two-electron, one-proton process that takes place at the electrode surface. If direct electroreduction was a plausible reaction route, then palladization of electrode surfaces should be of little relevance. Combination of TCE dechlorination at palladium surfaces and at palladium-substrate interface is a possible removal route. The use of palladized foam cathode influences TCE removal due to: distribution of Pd catalyst within high surface area, more hydrogen produced and larger surface area allowing compound interaction with Pd sites.

3.2. The three electrode system for TCE removal

The increased cathode area and Pd catalyst were applied to improve reduction in the three electrode system (Fe/Fe/MMO: C \rightarrow C \rightarrow A). The removal efficacy and pseudo-first rate constants for TCE degradation are given in Table 4. The use of the foam cathode in the three electrode system doubled TCE removal rate compared to the two electrode system but the removal efficiency was the same.

The influence of different Pd/Al catalyst positions (E1 or E2), amounts (g) and supporting materials on TCE degradation was tested (Fig. 7). In the absence of the Pd catalyst, 89% of TCE degraded (Table 3) while more than 99% TCE was removed regardless of the catalyst position. However, the removal rate constants differed depending on Pd catalyst position (Table 4). The E2 iron cathode polarization (the side parallel to E1 acts as anode) influenced the hydrogen evolution and therefore also influenced the Pd catalyst activity on TCE removal. Further experiments were conducted with the Pd catalyst on the E1 cathode. The enhanced performance of the three electrode system with Pd/Al catalyst compared to the system with two electrodes is due to both increased cathode surface area and ability to control the conditions for HDC. Current splitting between the cathodes caused generation of lower size hydrogen bubbles [64] at each electrode surface, which sufficiently interacted with the Pd sites at the catalyst surface.

The same TCE removal efficiency was achieved (more than 99%) when 2 g (10 mg Pd) and 5 g (25 mg Pd) of Pd/Al catalyst were used. However, the TCE removal rate was faster in the presence of 5 g Pd/Al catalyst (Table 3). This was due to the increased surface area of Pd catalyst and the Pd sites available for the reaction. Further increase in the catalyst amount caused significant increase in electrical resistance.

The influence of Pd catalyst supporting material on TCE degradation in the three electrode system was examined (Fig. 8). The results indicated that TCE degradation (more than 99%) was significantly faster when supported by Pd/C than Pd/Al. The same behavior was noticed in the system with two electrodes. Additionally, TCE reduction by palladized iron foam cathode (as E1) was investigated. The same final removal efficiency was achieved when Pd/Al, Pd/C and palladized foam cathode was used. The use of Pd catalyst on each tested supporting material resulted in higher final TCE removal

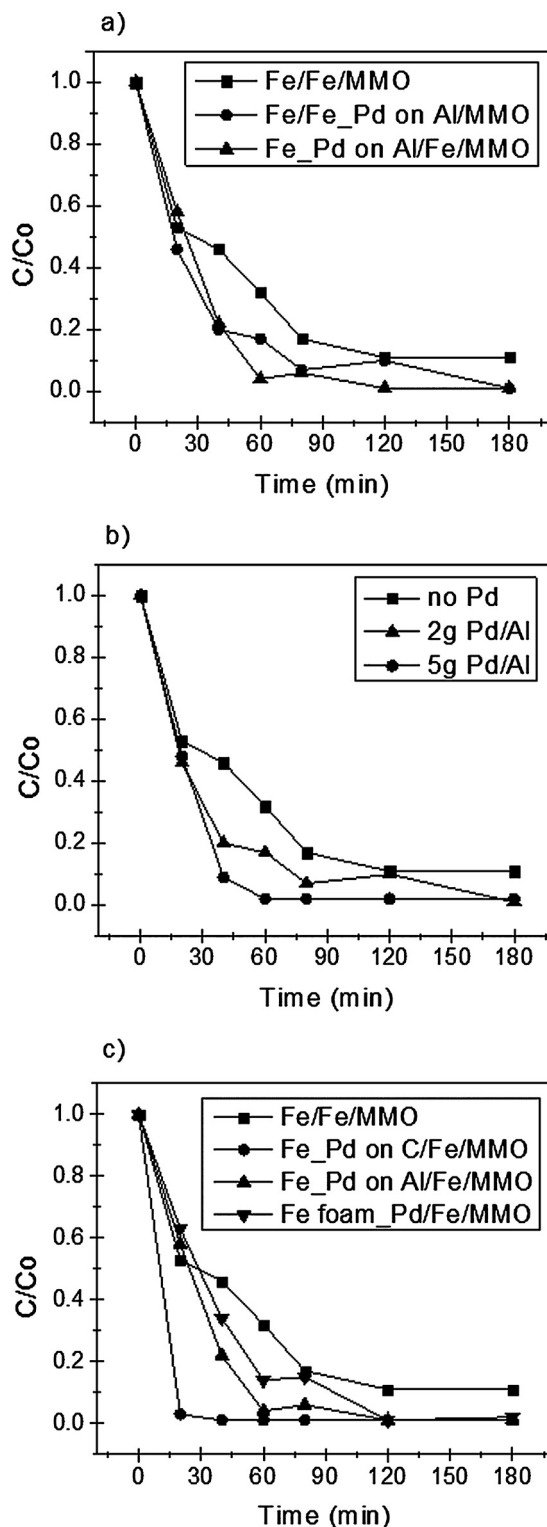


Fig. 7. The influence of Pd catalyst position (a), amount (b) and supporting material (c) in C \rightarrow A setup.

efficiencies and removal rates when applied in the three electrode system compared to the two electrode setup.

4. Conclusions

In this study we optimize the electrode sequence to promote hydrodechlorination of TCE in a mixed flow-through electrochem-

ical cell. The results show that a cathode followed by an anode positively affects TCE removal rate (2.2 times) and efficacy (by 26%) over the anode followed by cathode setup. Placing the anode downstream of the cathode minimizes the influence of oxygen generated at the MMO anode on TCE reduction at the cathode. Therefore, MMO anode can be used in a mixed flow-through cell without affecting TCE reduction. In addition, MMO anode in the C → A setup maintains initial the redox potential and pH values for the treated solution. Under the C → A arrangement, the TCE mass flux reduction rate increases with increasing flow velocity. Multiple cathodes that are used to increase the retention time in the reduction zone and iron foam cathode, utilized to magnify the cathode surface area, leading to an increased rate of TCE removal. More than 99% of TCE was removed in the presence of Pd catalyst on the carbon electrode and as an iron foam cathode coating in the C → A setup.

Acknowledgements

This work was supported by the US National Institute of Environmental Health Sciences (NIEHS, Grant No. P42ES017198). The content is solely the responsibility of the authors and does not necessarily represent the official views of the NIEHS or the National Institutes of Health.

References

- [1] M.J. Moran, J.S. Zogorski, P.J. Squillace, *Environ. Sci. Technol.* 41 (2007) 74–81.
- [2] USEPA, 2007, <http://nepis.epa.gov/Adobe/PDF/60000GJ1.pdf>
- [3] J. Hara, in: T. Puzyn (Ed.) *InTech*, 2012, Available from: <http://www.intechopen.com/books/organic-pollutants-ten-years-after-the-stockholm-convention-environmental-and-analytical-update/chemical-degradation-of-chlorinated-organic-pollutants-for-in-situ-remediation-and-evaluation-of-nat>
- [4] E.S. Semkiw, M.J. Barcelona, *Ground Wat. Monit. Rev.* 31 (2011) 68–78.
- [5] A. Tiehm, K.R. Schmidt, *Curr. Opin. Biotech.* 22 (2011) 415–421.
- [6] M. Farooq, I.A. Raja, A. Pervez, *Sol. Energy* 83 (2009) 1527–1533.
- [7] H. Che, S. Bae, W. Lee, J. Hazard. Mater. 185 (2011) 1355–1361.
- [8] M. Rashid, C. Sato, *J. Environ. Eng.* 138 (2012) 1179–1185.
- [9] O. Ayyildiz, R.W. Peters, P.R. Anderson, *Ultrason. Sonochem.* 14 (2007) 163–172.
- [10] H. Destailats, T.W. Alderson, M.R. Hoffmann, *Environ. Sci. Technol.* 35 (2001) 3019–3024.
- [11] M.A. Petersen, T.C. Sale, K.F. Reardon, *Chemosphere* 67 (2007) 1573–1581.
- [12] E.J. Petersen, R.A. Pinto, X. Shi, Q. Huang, *J. Hazard. Mater.* 243 (2012) 73–79.
- [13] D.H. Phillips, T. Van Nooten, L. Bastiaens, M.I. Russell, K. Dickson, S. Plant, J.M.E. Ahad, T. Newton, T. Elliot, R.M. Kalin, *Environ. Sci. Technol.* 44 (2010) 3861–3869.
- [14] C. Liu, D. Tseng, C. Wang, *J. Hazard. Mater. B* 136 (2006) 706–713.
- [15] F. Li, C. Vipulanandan, K.K. Mohanty, *Colloids surf. A: Physicochem Eng. Aspects* 223 (2003) 103–112.
- [16] K. Choi, W. Lee, *J. Hazard. Mater.* 211–212 (2012) 146–153.
- [17] C.J. Lin, Y.H. Liou, S. Lo, *Chemosphere* 74 (2009) 314–319.
- [18] L. Wu, S.M.C. Ritchie, *Chemosphere* 63 (2006) 285–292.
- [19] G. Lowry, M. Reinhard, *Environ. Sci. Technol.* 35 (2001) 696–702.
- [20] R. Muftikian, Q. Fernando, N. Korte, *Water Res.* (1995) 2434–2439.
- [21] F. He, D. Zhao, J. Liu, C.B. Roberts, *Ind. Eng. Chem. Res.* 46 (2007) 29–34.
- [22] H. Ma, Y. Huang, M. Shen, R. Guo, X. Cao, X. Shi, *J. Hazard. Mater.* 211–212 (2012) 349–356.
- [23] T.T. Tsai, C.M. Kao, J.Y. Wang, *Chemosphere* 83 (2011) 687–692.
- [24] Z. Yue-hua, X. Chun-Mei, G. Chang-Hong, *Procedia Environ. Sci.* 10 (2011) 1668–1673.
- [25] Y. Lee, W. Lee, *J. Hazard. Mater.* 178 (2010) 187–193.
- [26] R.H. Waldemer, P.G. Tratnyek, R.L. Johnson, J.T. Nurmi, *Environ. Sci. Technol.* 41 (2007) 1010–1015.
- [27] A.L. Teel, C.R. Warberg, D.A. Atkinson, R.J. Watts, *Water Res.* 35 (2001) 977–984.
- [28] S. Yamazaki, S. Matsunaga, K. Hori, *Water Res.* 35 (2001) 1022–1028.
- [29] S.H. Yuan, M.J. Chen, X.H. Mao, A.N. Alshawabkeh, *Water Res.* 47 (2013) 269–278.
- [30] S.H. Yuan, X.H. Mao, A.N. Alshawabkeh, *Environ. Sci. Technol.* 46 (2012) 3398–3405.
- [31] P. Lakshminathiraj, G. Bhaskar Raju, Y. Sakai, Y. Takuma, A. Yamasaki, S. Kato, T. Kojima, *Chem. Eng. J.* 198–199 (2012) 211–218.
- [32] D.M. Gilbert, T.C. Sale, *Environ. Sci. Technol.* 39 (2005) 9270–9277.
- [33] X.H. Mao, A. Ciblak, M. Amiri, A.N. Alshawabkeh, *Environ. Sci. Technol.* 45 (2011) 6517–6523.
- [34] X.H. Mao, S.H. Yuan, N. Fallahpour, A. Ciblak, J. Howard, I. Padilla, R. Loch-Carusio, A.N. Alshawabkeh, *Environ. Sci. Technol.* 46 (2012) 12003–12011.
- [35] X.H. Mao, A. Ciblak, K. Baek, M. Amiri, R. Loch-Carusio, A.N. Alshawabkeh, *Water Res.* 46 (2012) 1847–1857.
- [36] D. Mishra, Z. Liao, J. Farrell, *Environ. Sci. Technol.* 42 (2008) 9344–9349.
- [37] T. Li, J. Farrell, *Environ. Sci. Technol.* 34 (2000) 173–179.
- [38] S. Rondinini, A. Vertova, *Electrochemistry for the Environment*, in: C. Comninellis, G. Chen (Eds.), Springer, 2010, pp. 279–309.
- [39] J.H. Brewster, 1954, *J. Am. Chem. Soc.* 76 (1954) 6361–6363.
- [40] D.F. Call, M.D. Merrill, B.E. Logan, *Environ. Sci. Technol.* 43 (2009) 2179–2183.
- [41] N. Hoshi, K. Sasaki, S. Hashimoto, Y. Hori, *J. Electroanal. Chem.* 568 (2004) 267–271.
- [42] S. Rondinini, P.R. Mussini, P. Muttini, G. Sello, *Electrochim. Acta* 46 (2001) 3245–3258.
- [43] Y.H. Xu, Y.H. Zhu, F.M. Zhao, C.A. Ma, *Appl. Catal. A: Gen.* 324 (2007) 83–86.
- [44] I.F. Cheng, Q. Fernando, N. Korte, *Environ. Sci. Technol.* 31 (1997) 1074–1078.
- [45] H. Cheng, K. Scott, P.A. Christensen, *J. Electrochem. Soc.* 150 (2003) D25–D29.
- [46] C. Iwakura, Y. Tsuchiyama, K. Higashiyama, E. Higuchi, H. Inoue, *J. Electrochem. Soc.* 151 (2004) D1–D5.
- [47] B. Yang, G. Yu, D. Shuai, *Chemosphere* 67 (2007) 1361–1367.
- [48] V. Saez, M.D. Esclapez, I. Tudela, P. Bonete, J. Gonzalez-Garcia, *Ind. Eng. Chem. Res.* 49 (2010) 4123–4131.
- [49] W. Xie, S. Yuan, X. Mao, W. Hu, P. Liao, M. Tong, A.N. Alshawabkeh, *Water Res.* 47 (2013) 3573–3582.
- [50] G. Chen, E.A. Betterton, R.G. Arnold, W.P. Ela, *J. Appl. Electrochem.* 33 (2003) 161–169.
- [51] Y. Roh, K. Cho, S. Lee, *J. Environ. Sci. Health A* 36 (2001) 923–933.
- [52] G.N. Jovanovic, P. Plazl, P. Sakrithichai, K. Al-Khaldi, *Ind. Eng. Chem. Res.* 44 (2005) 5099–5106.
- [53] H. Li, The 5th International Conference on Bioinformatics and Biomedical Engineering (iCBBE 2011) (2015), <http://dx.doi.org/10.1109/icbbe.2011.5781080>.
- [54] L.J. Rajic, N. Fallahpour, S. Yuan, A.N. Alshawabkeh, *Water Res.* 67 (2014) 267–275.
- [55] A.N. Alshawabkeh, *Sep. Sci. Technol.* 44 (2009) 2171–2187.
- [56] A.N. Alshawabkeh, H. Sarahney, *Environ. Sci. Technol.* 39 (2005) 5837–5843.
- [57] D.M. Gilbert, T. Sale, M.A. Petersen, *In Situ Remediation of Chlorinated Solvent Plumes*, in: H.F. Stroo, C.H. Ward (Eds.), Springer Science + Business Media, LLC, 2010, pp. 573–590.
- [58] O. Scialdone, A. Gallia, L. Gurreri, S. Randazzo, *Electrochim. Acta* 55 (2010) 701–708.
- [59] C. Yan-qing, W. Zu-cheng, T. Tian-en, *J. Zhejiang Univ. Sci.* 6B (2005) 563–568.
- [60] B. Marselli, J. Garcia-Gomez, P.A. Michaud, M.A. Rodrigo, C. Comninellis, *J. Electrochem. Soc.* 150 (2003) D79–D83.
- [61] G. Chen, *Sep. Purif. Technol.* 38 (2004) 11–41.
- [62] D. Ghosh, C.R. Medhi, H. Solanki, M.K. Purkait, *J. Environ. Prot. Sci.* 2 (2008) 25–35.
- [63] D.B. Gent, A.H. Wani, J.L. Davis, A. Alshawabkeh, *Environ. Sci. Technol.* 43 (2009) 6301–6307.
- [64] R. Wuthrich, C. Comninellis, H. Bleuler, *Electrochim. Acta* 50 (2005) 5242–5246.
- [65] L. Gomez-Sainero, X.L. Seoane, J.L.G. Fierro, A. Arcoya, *J. Catal.* 209 (2002) 279–288.
- [66] F.D. Kopinke, K. Mackenzie, R. Koehler, A. Georgi, *Appl. Catal. A Gen.* 271 (2004) 119–128.
- [67] Y.I. Matatov-Meytal, M. Sheintuch, *Ind. Eng. Chem. Res.* 37 (1998) 309–326.
- [68] T. Karanfil, S.A. Dastghei, *Environ. Sci. Technol.* 38 (2004) 5834–5841.